Exceptional loss in ozone in the Arctic winter/spring 2020

Jayanarayanan Kuttippurath[1]*, Wuhu Feng[2,3], Rolf Müller[4], Pankaj Kumar[1], Sarath Raj[1],
Gopalakrishna Pillai Gopikrishnan[1], Raina Roy[5]

[1]CORAL, Indian Institute of Technology Kharagpur, Kharagpur–721302, India.
[2] National Centre for Atmospheric Science, University of Leeds, Leeds, LS2 9PH, UK
[3] School of Earth and Environment, University of Leeds, Leeds, LS2 9JT, UK
[4]Forschungszentrum Jülich GmbH (IEK-7), 52425 Jülich, Germany
[5]Department of Physical Oceanography, Cochin University of Science and Technology, Kochi, India

Correspondence to: Jayanarayanan Kuttippurath (jayan@coral.iitkgp.ac.in)

Abstract. Severe vortex-wide ozone loss in the Arctic would expose both ecosystems and several millions of people to unhealthy ultra-violet radiation levels. Adding to these worries, and extreme events as the harbingers of climate change, exceptionally low ozone with column values below 220 DU occurred over the Arctic in March and April 2020. Sporadic occurrences of low ozone with less than 220 DU at different regions of vortex for almost three weeks were found for the first time in the observed history in the Arctic. Furthermore, a large ozone loss of about 2.0–3.4 ppmv triggered by an unprecedented chlorine activation (1.5–2.2 ppbv) matching the levels occurring in the Antarctic was also observed. The polar processing situation led to the first-ever appearance of loss saturation in the Arctic. Apart from these, there were also ozone-mini holes in December 2019 and January 2020 driven by atmospheric dynamics. The large loss in ozone in the colder Arctic winters is intriguing, and demands rigorous monitoring of the region.

1 Introduction

Apart from its significance of shielding the harmful ultra-violet (UV) radiation reaching the surface of earth, stratospheric ozone is a key component in regulating the climate (e.g. Riese, et al., 2012). Changes in stratospheric ozone are always a big concern for both public health and climate (WMO, 2018; Bais et al., 2019). Due to unbridled emissions of Ozone Depleting Substances (ODS) to the atmosphere since the 1930s stratospheric chlorine peaked in the polar stratosphere in the early 2000s (Newman et al., 2007; Engel et al., 2018; WMO, 2018). The first signatures of polar ozone loss appeared over Antarctica by the late 1970s (Chubachi et al., 1984; Farman et al., 1985), and it peaked to saturation levels in the late 1980s due to already high levels of stratospheric chlorine (Kuttippurath et al., 2018). Recent studies have demonstrated the effectiveness of Montreal Protocol and its amendments and adjustments in reducing halogen gases, with a corresponding positive trend in ozone in Antarctica (Salby et al., 2011; Kuttippurath et al., 2013; Solomon et al., 2016; Chipperfield et al., 2017) and in northern mid-

latitudes (Steinbrecht et al., 2014; Nair et al., 2015; Weber et al., 2018). However, a positive trend in the Arctic ozone is not reported yet possibly because of the large dynamically driven inter-annual variability of ozone there (Kivi et al., 2013; WMO, 2018).

Antarctic winters are very cold and the ozone hole is a common feature of these winters since the late 1970s. There were winters with very low stratospheric temperatures with a stronger vortex that showed relatively larger loss in ozone, such as the winters of 1996, 2000, 2003, 2006 and 2015 (Bodeker et al., 2005; Chipperfield et al., 2017). There were also winters with high temperatures and smaller ozone losses as in the case of 1998, 2002, 2012 and 2019 (Müller et al., 2008; de Laat et al., 2010; Kuttippurath et al., 2015). Yet, the inter-annual variability of ozone loss in the Antarctic is very small in recent decades. On the other hand, colder winters with large losses of ozone (e.g. > 1.5 ppmv of loss) are rare in the Arctic (Rex et al., 2015, von der Gathen et al., 2021). The ozone loss derived from satellite and ozonesonde measurements show that most winters have ozone loss in the range of 0.5-1.5 ppmv and extremely cold winters showed large loss of about 1.5–2.0 ppmv (Manney et al., 2003; Kuttippurath et al., 2013; Livesey et al., 2015). Similarly, the ground-based measurements show about 15–20% of loss in most Antarctic winters, but the winters 1995, 1996, 2000, 2005 and 2011 were very cold with large loss of ozone, up to 25–30% (Goutail et al., 2005; Pommereau et al., 2018). However, these ozone loss values are still smaller than the 40–55% loss occurrence in the Antarctic (Kuttippurath et al., 2013; Pommereau et al., 2018).

The Arctic vortex is relatively short-lived (i.e. three to four months). The vortex normally strengthens by mid-December or early January and dissipates by mid-March. Major and minor warmings are common features of Arctic winters. The Arctic vortex in any winter would be frequently disturbed by planetary waves that emanate from the troposphere. In general, planetary wave numbers 1, 2 and 3 are mostly responsible for the momentum transfer to the stratosphere. This dynamical activity would increase the temperature in the lower stratosphere and trigger stratospheric warmings. The warmings can be minor or major, depending on the strength of wave activity, increasing the polar temperature and eventually disturbing the polar vortex. The vortex can be distorted, displaced, elongated and even split in two in accordance with the potency of momentum imparted by the waves. When the polar vortex is disturbed, the ozone loss will be smaller and the final warming can be as early as in late February or early March, as for many Arctic winters (e.g. Manney et al., 2003; Kuttippurath et al., 2012; Goutail et al., 2015). However, the vortex dissipates and chemical ozone loss terminates when a major warming occurs there. In an earlier study, Kuttippurath et al. (2012) observed an increasing trend in major warmings, and ozone loss is found to be proportional to the timing of the major warmings, as early winter warmings stop polar stratospheric cloud (PSC) formation (i.e. stop the action of heterogeneous chemistry) because of the higher temperatures. This situation limits the activated chlorine available for ozone loss and results in smaller loss in warm Arctic winters. Since 1979, during the satellite era, there were two extreme winters with large loss of ozone in the Arctic; 2005 and 2011 (Coy et al., 1997; Feng et al., 2007; Horowitz et al., 2011). The occurrence of extreme events is a feature of climate change (e.g. IPCC, 2007). Therefore, the extremely cold winters with large loss in ozone could also be a harbinger of climate change. Previous studies have postulated that the cold winters will get even colder

1

67 with large loss in ozone (Sinnhuber et al., 2000; Rex et al., 2004; Chipperfield et al., 2005; Rider et al., 2013, von der Gathen

68 et al., 2021). Analyses of the past colder Arctic winters indicate that it is likely that the colder winters may experience large

69 loss in ozone, as in the case of 2005, 2016 and 2011. There are already studies on this winter discussing the ozone loss and

70 meteorology (Manney et al., 2020; Wholtmann et al., 2020; Rao and Grafinkel, 2020; Weber et al., 2021; Innes et al., 2021;

71 Wilka et al., 2021; Grooß and Müller, 2021; von der Gathen et al., 2021; Feng et al., 2021). However, in this study, we use

72 different data sets, different loss estimation methods, and several assessment parameters together to study the polar processing

73 and ozone loss in the Arctic winter 2020, and such an analysis is never done for this winter. This is particularly important as

74 the winter was very cold with the largest ozone loss in the observational record and experienced the total column ozone (TCO)

75 values below 220 DU for several days in the vortex, for the first time.

76 **2 Data and Methods**

77 We have used two satellite ozone profile datasets. The level 2 data from the

78 (i)   Microwave Limb Sounder (MLS) v4.2 and

79 (ii)   Ozone Mapping and Profiler Suite (OMPS) v2.5 (ozone).

80 (iii)   We have also used the ozonesonde measurements from the Arctic stations at Alert (62.34° N, 82.49° W) and Eureka

81 (79.99° N, 85.90° W). The ozonesonde measurements have an uncertainty of 5–10% (Smit et al., 2007).

82

83 Three satellite-based total column ozone (TCO) data are also employed (level 3) for our analyses

84 (iv)   Ozone Monitoring Instrument (OMI, DOAS v003),

85 (v)   OMPS (v2.1),

86 (vi)   Global Ozone Monitoring Experiment (GOME) 2 (GDP4.8),

87 (vii)   Modern-Era Retrospective analysis for Research and Applications (MERRA)-2 and

88 (viii)   Brewer spectrometers from Alert and Eureka.

89

90 These TCO measurements have an uncertainty of 2–5%. The ozone and other trace gas profiles are provided in pressure

91 coordinates, which are converted to isentropic coordinates using the temperature data from the same satellite, except for OMPS,

92 for which the temperature data are taken from ERA5. We use the European Centre for Medium-Range Weather Forecasts

93 (ECMWF) Reanalyses ERA5 potential vorticity (PV) on a 1°×1° grid to determine the vortex edge. The PV data are also

94 converted to isentropic coordinates using the ERA5 temperature data. We computed the equivalent latitude at each isentropic

95 level at 5 K intervals from 350 to 800 K, which is then used to compute the vortex edge using the Nash et al. (1996) criterion.

96 We use measurements inside the polar vortex for the ozone loss analysis. The missing values in satellite measurements were

97 filled with linear interpolation.

98

99   We have taken ozone, ClO, HNO₃ and N₂O from the Aura MLS measurements. The ozone measurements at 240 GHz have a

100   vertical resolution of 2–3 km, vertical range of 261–0.02 hPa and an accuracy of 0.1–0.4 ppmv. The vertical range of HNO_3

101   measurements is 215–1.5 hPa, vertical resolution is 2–4 km, with an accuracy of 0.1–2.4 ppbv, depending on altitude. The

102   N_2O measurements are available for the 68–0.46 hPa vertical range, and 68 hPa roughly equivalent to the 400 K isentropic

103   level. The data were extrapolated up to 350 K by performing exponential fitting to N_2O vertical distribution at 400–600 K by

104   considering the exponential change of N_2O with altitude. The accuracy of retrievals at 190 GHz is about 2–55 ppbv at this

105   altitude range and the vertical resolution is about 2.5–3 km. The vertical resolution of ClO measurements at 640 GHz is about

106   3–3.5 km over 147–1 hPa, and the accuracy of measurements is about 0.2–0.4 ppbv. The measurements also have latitude-

107   dependent bias of about 0.2–0.4 ppbv, depending on altitude (Livesey et al., 2013; Santee et al., 2008; Froidevaux et al., 2008).

108

109   The OMPS consists of three sensors that measure scattered solar radiances in overlapping spectral ranges and scan the same

110   air masses within 10 min. The nadir measurements are used to retrieve ozone total column and vertical profiles (NP). The

111   Limb Profiler (LP) measures profiles with high vertical resolution (∼ 2–3 km) and the LP retrievals are in good agreement

112   with other satellite measurements and the differences are mostly within 10% (Kramarova et al., 2018). The OMPS TCO shows

113   0.6–1.0% differences with Brewer and Dobson ground-based TCO measurements across the latitudes, and are also biased +2%

114   when the TCO is above 220 DU (Bais et al., 2014). GOME-2 was flown on MetOp-A satellite in 2006. The GOME-2 ozone

115   column has a positive bias in the northern high latitudes of about 0.5–3.5% (Layola et al., 2011). The OMI TCO measurements

116   have an accuracy of about 5% in the polar regions (Kroon et al., 2008; Kuttippurath et al., 2018). The Brewer spectrometers

117   operate in the UV region and their ozone observations have an accuracy of about 5%.

118

119   The ozone loss is estimated using two different methods and four different data sets to make sure the analyses are robust. The

120   first method used is the widely used profile descent method, wherein the N_2O data are used for the calculations of air mass

121   descent in the polar vortex. The reference profile of N_2O was taken from the month of December, and therefore, the loss

122   calculations are presented from December (May for Antarctic) onwards. The second method used for the calculation of ozone

123   is the passive tracer method, for which a passive odd-oxygen tracer is simulated using a CTM (Chemical Transport Model)

124   and is subtracted from the measured ozone to determine the ozone loss, as the changes in tracer are modulated only by the

125   dynamics (Feng et al., 2005). We have used the SLIMCAT model for the tracer calculations (Chipperfield, 2006) and

126   investigated the Arctic ozone loss under different meteorological conditions including Arctic winter/spring 2020 (e.g.,

127   Chipperfield et al., 2005; Bognar et al., 2021; Feng et al., 2021; Weber et al., 2021).

3. Results and discussion

3.1 The exceptional meteorology of the Arctic winter/spring 2020

Figure 1 shows the times series of stratospheric meteorology in the Arctic winter/spring 2020 compared to that long-lasting polar vortex years 1997 and 2011. Time series of the meteorological parameters for all Arctic winters since 1979 are also shown (grey coloured curves) for comparison. In general, the temperatures are between 210 and 195 K. In 2020, the temperatures were about 195 K in December, 190–195 K in January–March and 195–205 K in April. However, the minimum temperature in late winter 2020 is generally lower than 195 K, lasting about 115 days from December through early April. The temperatures are general lower than those in the 2011 winter, and those in late March and April are the lowest on the observational record. The lower temperatures in late December through mid-March are key to PSCs, chlorine activation, the maintenance of high values of active chlorine and ozone loss. Low temperatures are thus a common phenomenon in winters with large loss of ozone (e.g. 1995, 2000, 2005 and 2011). Therefore, the higher temperatures in early winter and limited chlorine activation were the reason for relatively smaller ozone loss in 1997; although it was a winter with a strong vortex up to the end of April (Coy et al., 1997; Feng et al., 2007; Kuttippurath et al., 2012). Since minor warmings (mWs) are very common in the Arctic winters, we also examined the occurrence of mW events by checking the temperature at 90° (North Pole) and 60° N at 10 hPa and zonal winds at 60° N at 10 hPa. The analyses show a small increase in temperature on 5 February 2020 (i.e. a minor warming) and a corresponding change in zonal winds.

The temperatures were consistently lower than the nitric acid trihydrate (NAT) equilibirum threshold of about 195 K and therefore, large areas of Polar Stratospheric Clouds (PSCs) are observed from December to mid-February. Even though PSCs may also be composed of liquid particles and not only NAT (e.g. Pitts et al. 2009; Spang et al., 2018), the NAT equilibrium threshold constitutes a good estimate for the occurrence of heterogeneous chemistry (e.g. Grooß and Müller, 2021; von der Gathen et al., 2021). The potential PSC area (APSC) was about 4 million km^2 in December 2020 at 460 K, but it doubled in January through mid-March. The APSC from mid-February to late March is also largest on the observational record (Figure 1). The low temperatures (i.e. lower than 188 K) also produced a very high amount of ice PSCs at the end of January and early February (up to 4 million km^2) when the lowest temperatures in 40 years were recorded in the Arctic. This is the largest ice PSC ever observed in terms of its area, volume and number of days of appearance (i.e. frequency) in the Arctic and the area is twice that of the winter 2011 (also see Deland et al., 2020). The PSC area shrunk to half of its area in late January and February, as the lower stratospheric temperature increased during the period. This was the only occasion that the temperature increased and PSC areas limited to below 4 million km^2 in the winter 2020. Note that the PSC area and volume were largest in 2016, not in 2020 (Figure S1) (Kirner et al., 2015).

The potential vorticity (PV) at ~17 km (about 460 K potential temperature level) show that the polar vortex was very strong in the lower stratosphere in 2020. The PV values were consistently higher than the previous cold (i.e. 1995, 2000, 2005 and

161 2011) and long lasting (e.g. 1997 and 2011) winters in March and April. This indicates that the winter 2020 had the strongest

162 vortex in the recent history, as demonstrated by the PV time series of different Arctic winters (Figure 1, second panel, left).

163 However, the zonal winds were strongest in 1997 during the March-April period. The diagnosis with heat flux and the eddy

164 heat flux associated with waves demonstrates that the momentum transported from the troposphere to stratosphere was very

165 weak in 2020 (in the range of -20 to 30 Km s^{-1}), and the heat flux values are zero or negative (e.g. -10 Km s^{-1} in February)

166 during most part of the winter. These results are also in agreement with the eddy heat flux computed for the waves, as they

167 also show smaller wave momentum to the stratosphere. In short, the eddy heat flux and wave heat flux show smaller values in

168 January-April; indicating the reason for the less disturbed long-lasting vortex in 2020. According to Lawrence et al. (2020),

169 apart from the weak tropospheric forcing, the formation of reflective configuration of stratospheric circulation was another

170 factor that aided in the strengthening of the vortex in 2020.

171

172 The potential vorticity analyses show a strong and large vortex in early December. The vortex began to grow and occupied the

173 entire polar region (defined by PV vortex edge) by early January, as shown in Figure 2. The lowest temperatures of the past

174 40 years were recorded by the end of January and the vortex was exceptionally strong and large (e.g. Wohltmann et al., 2020;

175 Rao and Garfinkel, 2020). The mW distorted and elongated the vortex in early February, but the vortex was still strong and

176 continued to be intact until the last week of April 2020. The extraordinary persistence of a strong and undisturbed Arctic vortex

177 in March and April is evident in the PV maps. We also examined the Arctic winters since 1979 in terms of their dynamical

178 activity, as shown in Figure S1b. The analyses show that, although the average vortex temperature and vortex area at 70 hPa

179 was not very exceptional, the westerly winds (25 ms^{-1}) were strongest and dynamical activity was weakest (with heat flux 17

180 K ms^{-1}) in the past twenty years. This further suggests that the winter 2020 was unique and that wave forcing was very weak

181 during the period.

3. 2 Strong air mass descent and associated ozone distribution

183 Figure 3 shows the distribution of ozone, ClO, N$_2$O, HNO$_3$ and the ozone loss estimated for the winter 2020 using satellite

184 observations. We use the measurements from MLS on the Aura satellite (Livesey et al., 2015). The MLS data has been widely

185 used for the study of polar ozone loss, as the instrument provides measurements of some key ozone-related chemistry trace

186 gases such as ClO, N$_2$O and HNO$_3$ to delineate the features of chlorine activation, vortex descent and denitrification,

187 respectively (Manney et al., 2020). The ozone distributions in the vortex show < 1.0 ppmv in December, slightly higher values

188 of about 1.5 ppmv in February and smaller than 1.0 ppmv from Mid-March to the end of April at 400 K. The measurements

189 show exceptionally low values of ozone, about 0.5 ppmv or below, during the period mid-March through to the end of April

190 at 350–450 K. The ozone values show < 2.5 ppmv from December to mid-January, < 2 ppmv January and February and < 1.0

191 ppmv in March-April at 350–450 K, and about 2–4 ppmv above 500 K; suggesting an unusual chemical depletion of ozone in

192 December and late January. The ozone values are about 3–4 ppm above 550 K throughout the winter; implying little reduction

193 in ozone there. The unusual feature here is the extremely small ozone mixing ratios of 1.0 ppmv in early December and March–

1

194 April below 450 K (about 16 km). This reveals huge depletion of ozone in the lower stratosphere and therefore, we have

195 quantified the ozone loss for the winter. We use the profile descent method using the trace of air motions N_2O and is a widely

196 used method for ozone loss estimation (Bremer et al., 2002; Rex et al., 2002; Jin et al., 2006).

197

198 For instance, the MLS measurements show that N_2O values were 250 ppbv at 400 K, 150 ppbv at 500 K and 50 ppbv at 600

199 K in December. The N_2O observations show strong air mass descent with values down to 100 ppbv at 400 K and about 25–50

200 ppbv above 500 K in early February. Again, N_2O values exhibit below 50 ppbv in late March at 400 K. The N_2O distributions

201 show below 50 ppbv at all altitudes from early February onwards; suggesting substantial dynamic descent in the stratosphere.

202 When a particular altitude is considered, e.g. the 450 K potential temperature level, the N_2O values show 160 ppbv in early

203 December, 100 ppbv in early January, 50 ppbv in early February and less than 50 ppbv thereafter. On the other hand, the N_2O

204 distributions show 50 ppbv in early December and below that value afterwards at 500 K. The severe air mass descent in this

205 winter is further depicted in Figure S2, where monthly correlations between ozone and N_2O are presented.

206 **3.3 Ozone loss and mini-holes in December and January**

207 There were vortex-wide PSC occurrences in the first week of December, about 2-4 million km^2 in area (APSC) and about 70

208 million km^3 in volume (VPSC) (see Rex et al., 2005 for their definitions). The APSC and VPSC dropped significantly

209 afterwards and then gradually increased again by mid-December to 10 and 120 million km^3, respectively. An unusual increase

210 in activated chlorine is observed during the first week of December in conjunction with the appearance of PSCs. The

211 temperatures began to decrease from 198 K in mid-December to 187 K by the end of January, as shown in Figure 1. The

212 chlorine activation peaked and showed record levels of ClO, about 1.5–2.0 ppbv at 400–600 K, during this period. The

213 chemical ozone loss began in early January with about 0.5 ppmv and increased to 1.5 ppmv by the end of January below 500

214 K. The loss above that altitude is always lower than 0.5 ppmv, which shows that the ozone loss is restricted to the altitudes

215 below 21 km (i.e. 550 K).

216

217 In general, the ozone loss starts in December in the middle stratosphere and then gradually progresses towards the lower

218 stratosphere by January. The loss would be below 0.5 ppmv in December and about 0.5–1.0 ppmv in January in the lower

219 stratosphere in cold Arctic winters. However, in the Arctic winter 2020, the ClO and ozone loss show unusually high values

220 of about 1.5–2.0 ppbv and 1.5–2.0 ppmv, respectively. Since ozone loss of this scale requires sunlight and high levels of ClO,

221 and there is no sunlight in the Arctic vortex in early winter, the appearance of huge amounts of ClO during this period is

222 surprising. The only possibility to have such high-levels of chlorine activation is the displacement of vortex to sunlit latitudes.

223 The analyses of vortex position in early December and late January (Figure 2) reveal that the vortex was at $55°–60°$ N.

224 Therefore, a strong polar vortex, very low temperatures, large volumes of PSCs and shift of vortex to the sunlight part of mid-

225 latitudes caused the unprecedented chlorine activation and ozone loss in the first week of December and late January. This is

226 similar as Arctic winter 2002/03 (e.g. Goutail et al., 2005; Kuttippurath et al., 2011).

1

227

228 In addition to the ozone loss inside the vortex, there is another interesting phenomenon in December and January. The analyses

229 of TCO show that there were Arctic ozone mini-holes (e.g. Stenke and Grewe, 2003; Rieder et al., 2013) of about 300–700

230 km^2 size in the first week of December (1–6 December 2019) and on 26 January 2020 (Figure 4). The lowest TCO measured

231 of the winter was also at the latter date. A detailed analysis with TCO, PV, temperature and ClO reveal that those ozone mini-

232 holes were dynamically driven, as there was rapid air mass transport to the southern Arctic in early December and late January.

233 These ozone mini-hole occurrences due to rapid changes in weather patterns and the total column ozone returns to the amount

234 of normal levels of ozone in few days

235

236 Ozone mini-holes are a dynamically driven sporadic decrease in TCO observed mostly in the mid-latitudes of both hemispheres

237 due to rearrangement of the ozone column associated with tropospheric weather systems (Reed, 1950). The mini-holes are

238 called so, as the TCO is less than 220 DU in those areas, and is one of the criteria defining the Antarctic ozone hole, although

239 they differ in the nature of formation and spatial extent. These transient spatial and temporal events were identified first by

240 Dobson and Harrison (1926) much before the identification of chemical ozone loss and were referred to as mini-holes by

241 Newman et al. (1988) and McKenna et al. (1989). The plunge in TCO results when, the horizontally advected ozone poor

242 tropospheric air mass interacts with the vertical air column motions in the anticyclonic ridging regions of the upper troposphere

243 in the polar regions. As a consequence of this divergence, mixing or both may result in the appearance of mini-holes (e.g.

244 Peters et al., 1995; James et al., 1997; Canziani et al., 2002). Since its identification, the criteria for the definition of mini-holes

245 differed based on the thresholds of TCO amounts and spatial coverage in different geographical locations (Millán and Manney,

246 2017). In our study the threshold is taken to be 220 DU (see Bojkov and Balis, 2001). Many studies have also analysed the

247 mini-hole formations in the northern hemisphere (e.g. James, 1998; Krzyścin, 2002; Stenke and Grewe, 2003; Feng, 2006).

248 Here, we analyse the ozone mini-holes that appeared in the polar region of the winter 2020 and their dynamical origin.

249

250 We used the HYSPLIT trajectory model to find the air mass transport at three different altitudes (17, 18 and 19 km) in the

251 lower stratosphere, where the mini-holes are found (Figure 4, right panels). The air mass exported from mid- and low latitudes

252 has very low PV values, low temperature and high ClO. It suggests that the TCO transported from mid-latitudes triggered the

253 ozone "holes" (ozone values < 220 DU). To further examine the low ozone values outside the vortex, we selected two

254 ozonesonde measurements in the region (Alert: 62.34° N, 82.49° W and Eureka: 79.99° N, 85.90° W), which are shown in

255 bottom panels of Fig. 4 for selected dates in December and January. These measurements show significant reduction in ozone

256 (Coy et al., 1997; Feng et al., 2007; Horowitz et al., 2011) between 12 and 18 km; confirming the findings from the satellite

257 total column measurements.

258

259 It should be mentioned that there was already large chemical loss of ozone inside the Arctic vortex in early December and late

260 January owing to the conventional polar ozone loss chemistry (as shown in Figure 3). However, the ozone mini-holes that

1

261 appeared outside the vortex were primarily caused by dynamics. We cross-checked TCO from OMI (Bias et al., 2014), OMPS

262 (Flynn et al., 2014), GOME-2 (Layola et al., 2011) and MERRA-2 (Gelaro et al., 2017), and found that the ozone mini-holes

263 were present in all these TCO datasets.

3.4 Prolonged chlorine activation and chemical ozone loss

265 When the Arctic winters are very cold, chlorine activation occurs in the Arctic lower stratosphere at 400–500 K in January and

266 February. In 2011, the chlorine activation was observed up to the end of February and was intermittent with a peak value of

267 about 1.6 ppbv, and was mostly at 400–500 K (e.g. Manney et al., 2011; Kuttippurath et al., 2012; Livesey et al., 2015; Griffin

268 et al., 2018). Conversely, in the Arctic winter 2020, there was continuous and sustained chlorine activation from December to

269 early April, except during the mW periods of mid-December and early February. The ClO values are also 0.5 ppbv larger than

270 those observed in the winter 2011. Feng et al. (2021) also stated that the chlorine activation in 2020 lasted longer than that in

271 2010/11. Therefore, strong chlorine activation was observed in March-April with ClO values of about 1.0–1.6 ppbv at 400–

272 550 K and the peak ClO value is about 2.1 ppbv.

273

274 The minor warming (Figure 1) caused a break in chlorine activation (Figure 3 for ClO) in early March. Nevertheless, the

275 temperature decreased shortly thereafter, which produced continued chlorine activation until early April at 400–550 K. The

276 ozone loss deepened in March and peaked by the end of March, and showed the maximum of about 1.5–3.4 ppmv at a broader

277 altitude range, up to 500 K. The ozone loss above that altitude (i.e. 550 K) was about 0.5–1 ppmv, which is still larger than

278 that that of any other Arctic winter. In fact, the loss of 1.0 ppmv is the peak loss observed in normal or moderately cold winters

279 of the Arctic (e.g. Kuttippurath et al., 2013); suggesting the severity of ozone loss even at the higher altitudes in this winter.

280 The maximum loss in 2020 was recorded at the end of March to the end of April, about 2.0–3.4 ppmv at 400–500 K and about

281 0.5–1.5 ppmv at 500–600 K. Furthermore, when compared to the early winter values, the late winter low HNO_3 values suggest

282 very severe denitrification, about 2–4 ppbv in the same period at 350–450 K (e.g. Manney et al., 2020). The HNO_3 values in

283 the lower stratosphere in March–April are about 60–80% lower than those of December–February at the same altitude levels

284 (Pommereau et al., 2018; Lindenmaier et al., 2012). The gravest denitrification was in December, with values of about 0–2

285 ppbv below 400 K and 4–6 ppbv at 400–450 K. Therefore, high chlorine activation and strong denitrification (as deduced from

286 the HNO_3 analyses shown in Figure 3) provided the basis for an unprecedented situation for large ozone loss of about 2–3.4

287 ppmv in the lower stratosphere in March–April.

288

289 Since the ozone loss in 2020 is exceptionally larger, we have employed another set of measurements to estimate ozone loss to

290 reconfirm that the derived results are robust. The loss estimated from OMPS measurements together with other analyses are

291 shown in Figure 5 (left). The maximum ozone loss profile extracted from the OMPS data shows very good agreement with

292 that from the MLS measurements for the Arctic winter 2020. The peak ozone loss values show about 2–2.8 ppmv in the lower

293 stratosphere below 550 K. Since the maximum ozone loss profiles are averaged for a few days, the loss values are slightly

294 lower than those from MLS. The lower stratosphere shows similar ozone loss values, but the loss above 500 K shows slightly

295 smaller values (0.1–0.5 ppmv) due to the low bias of OMPS measurements at these altitudes as compared to the MLS

296 measurements (Kramarova et al., 2018). The comparison with OMPS confirms that the method adopted for ozone loss is

297 robust. Our estimates are in good agreement with those of Manney et al. (2020), Weber et al. (2021) and Wohltmann et al.

298 (2020), who also derive a loss of about 2.1–2.8 ppmv below 450 K from the MLS measurements.

3. 5 The Arctic ozone loss in the context of other Arctic winters

300 Arctic winters are normally warmer that those in the Antarctic and occurrences of PSCs are sparse and infrequent. Therefore,

301 high chlorine activation and significant ozone loss is limited to winters with very low temperatures in December–February

302 (Tilmes et al., 2014; Goutail et al., 2005; WMO, 2018; Newman et al., 2008; Kuttippurath et al., 2012). The ozone loss observed

303 in warm winters (e.g. 2006 and 2009) is about 0.5–0.7 ppmv, moderately cold winters (e.g. 2008 and 2010) is about 1.0–1.2

304 ppmv and very cold winters (e.g. 2005) is 1.4–1.6 ppmv (e.g. WMO, 2018). However, the ozone loss in the winter 2011 was

305 about 1.0 ppmv (or 30–40 DU) larger than that of other Arctic winters (about 2.1–2.3 ppmv or 100–100 DU). This ozone loss

306 was similar to the loss found in warmer, more perturbed Antarctic winters (e.g. 1988 and 2002) (Manney et al., 2011;

307 Kuttippurath et al., 2012; Feng et al., 2015; Pommereau et al., 2018). We applied the same loss estimation method to the

308 measurements for the Arctic winter 2011 to compare with that of the Arctic winter 2020. This would also test the veracity of

309 the loss estimation procedure and the results are shown in Fig. 5.

311 The peak ozone loss in the Arctic winter 2011 is about 2.1 ppmv, which is in very good agreement with all other available

312 analyses for that winter (WMO, 2014, 2018; Griffin et al., 2018; Livesey et al., 2015). However, the ozone loss in the Arctic

313 winter 2020 is about 0.7 ppmv higher than that in 2011, about 2.8 ppmv. The difference in ozone loss between the winters is

314 negligible above 480 K. Therefore, it is evident that the ozone loss in the Arctic winter 2020 is the largest on the record and is

315 significantly higher than that of any previous Arctic winter. A very similar conclusion is also presented in the study of Grooß

316 and Müller (2021).

318 Furthermore, we applied another loss estimation method to test robustness of the extreme ozone loss values; the passive method

319 that uses a passive tracer (i.e. no chemistry) simulation. We have used the well-known and widely used TOMCAT/SLIMCAT

320 model simulations for the tracer calculations (Chipperfield et al., 1999; Dhomse et al., 2019). The ozone loss computed with

321 the passive method shows the peak value of about 2.3–2.5 ppmv at about 450 K in the Arctic winter 2020 (Figure 5, second

322 panel from the left). This ozone loss is slightly higher than that of the Arctic winter 2011, about 0.2 ppmv. It is also observed

323 that the ozone loss in 2020 is higher than that of 2011 below 475 K, but the loss estimated in the 2011 winter exceeds about

324 0.3–0.5 ppmv above 475 K up to 700 K (e.g. Manney et al., 2020; Wohltmann et al., 2020). However, these ozone loss

325 estimates are lower than those estimated with the descent method, by about 0.5–0.7 ppmv depending on altitude. The analysis

with ozone and N_2O from the model indicates that modelled ozone is higher than (by about 1–1.5 ppmv) the measurements at these altitudes, which could be due to the slower dynamical descent in the model.

It is clear that the ozone loss in 2020 is the largest among Arctic winters so far. Therefore, we also examined the evolution of chlorine activation in terms of the amount of ClO in each Arctic winter, as the total chlorine is decreasing in the stratosphere due to the effect of Montreal Protocol (e.g. Strahan et al., 2017; WMO, 2018; Dhomse et al., 2019) and we expect a corresponding response in ozone loss in the polar winters. Stratospheric halogen levels (EESC) in the Arctic in 2020 are more than 10% below the maximum levels in 2000 (Grooß und Müller, 2021). Figure 6 shows the MLS ClO observations, the December-February and December-March potential PSC areas, and EESC in each winter since 2005. The analyses show that the chlorine activation was very severe and continuous for about four months in 2020. However, the highest ClO and largest APSC values were observed in winter of 2016. Many cold winters showed ClO values around 1.8–2.0 ppbv as found in 2020, but the sustained chlorine activation that was observed in 2020 was unique. Although the high ClO values in March were also observed in 2011, the chlorine activation was not as severe as in 2020 in early winter (December–January). The record-breaking ice PSCs in the winter 2020 might have also contributed to the exceptional chlorine levels. On the other hand, the unprecedented chlorine activation observed in 2016 was more episodic, such as in mid-December, mid-January to early February and late February. Therefore, the continuous and severe chlorine activation from December through March was the key for the record-breaking ozone loss in 2020. Figure 6(b) and (c) further illustrate that the peak ClO profiles or the time series of average ClO for the entire winter will not reveal the depth of chlorine activation. We also looked at the changes in EESC during the period (2005-2020) and there has been continuous decline in EESC during the period (Fig. 6, top panel). The rate of change of EESC during the period is about 246.16 ppt per year (e.g. WMO, 2018); suggesting a consistent reduction in stratospheric halogen loading in 2020 (e.g. Grooß and Müller, 2021).

3.6 The Arctic ozone loss and the Antarctic ozone loss

The peak ozone loss in the Antarctic happens at around 500 K and the loss is severe from 400 to 600 K for five months continuously from August to November (Tilmes et al., 2006; Huck et al., 2005; Sonkaew et al., 2013; Kuttippurath et al., 2015). In contrast, the cold Arctic winters are normally shorter and maximum ozone loss occurs at around 425–475 K for a period of about two months, from mid-January to mid-March (e.g. Kuttippurath et al., 2010; Manney et al., 2004). The ozone loss in the Arctic is limited to the altitudes below 500 K. The ozone loss in the Arctic winter 2020 was very high, and therefore, we compare the Arctic ozone loss in 2020 with that in the Antarctic winters 2015 and 2019. The Antarctic winter 2015 was one of the coldest and 2019 was one of the warmest, and therefore, the assessment would give an upper and lower bound of ozone loss estimate for the Arctic winter 2020.

The peak ozone loss estimated using the vortex descent method is about 2.8 ppmv at 480 K in the Antarctic winter 2015 and about 2.3 ppmv at 490 K in 2019 (Figure 5). The ozone loss in the Antarctic winter 2015 shows consistently higher values

359 (about 0.1–0.5 ppmv) than that of 2019 up to 550 K, and the loss is similar above that altitude in both winters. The ozone loss

360 is about 1.0 ppmv at 370 K, 2.6 ppmv at 460 K, 1.5 ppmv at 550 K, 0.5 ppmv at 650 K and it terminates at 700 K in the

361 Antarctic winter 2015. In the Arctic winter 2020, the ozone loss shows about 0.3 ppmv at 370 K, 2.0 ppmv at 430 K and 480

362 K, 1.5 ppmv at 550 K and loss terminates above that altitude. The peak ozone loss is about 2.3 ppmv at 460–470 K. On the

363 other hand, the loss in the Antarctic winters above 470 K is very large and reaching up to 700 K. The peak ozone loss in the

364 Arctic winter 2020 is about 2.8 (2.3) ppmv and is at 460–470 K. This is also the main difference between the Arctic and

365 Antarctic ozone loss, as the broader and larger ozone loss occurs above the 470 K in the Antarctic. The difference is almost

366 1.0 ppmv above the peak ozone loss altitude. Therefore, the ozone loss in the Arctic winter 2020 is either equal or larger than

367 that of the Antarctic winter 2019 below 470 K, but the loss is smaller than that of the Antarctic winters above 525 K.

368

369 We have also applied the passive method to further examine the estimated loss in the Arctic and Antarctic winters (Figure 5,

370 second panel from the left). The ozone loss estimated with the passive method exhibits smaller values in the lower stratosphere

371 in comparison with that derived from the descent method. The loss is about 0.2 ppmv at 350 K, 1.6 ppmv at 400 K and 2.3

372 ppmv at 450 K in the Arctic winter 2020. The peak loss is recorded at 450–460 K and the loss decreases with altitude, about

373 1.5 ppmv at 500 K and 0.1 ppmv at 530 K. In the Antarctic winter 2019, the ozone loss shows similar values as that of the

374 Arctic winter 2020 at 370–420 K, but slightly smaller than that of the Arctic winter at 420–470 K. The maximum ozone loss

375 in Antarctic winter 2019 is estimated at 470 K, about 2.3 ppmv, and about 0.5–1.5 ppmv above that altitude, which is higher

376 than that of the Arctic winter 2020. Furthermore, the Arctic ozone loss halts at about 550 K, whereas the Antarctic ozone loss

377 at this altitude is as high as 1.5 ppmv. In the Antarctic winter 2015, the ozone loss is about 1.0 ppmv at 370 K, 2.0 ppmv at

378 400 K and the peak loss of about 2.8 ppmv at 475 K. The loss gradually decreases with altitude, such as 2.1 ppmv at 500 K,

379 1.5 ppmv at 550 K, 1.0 ppmv at 600 K and 0.5 ppmv at 650 K. The diagnosed ozone loss in the Antarctic winter 2015 is thus,

380 higher than that of the Antarctic winter 2019 and the Arctic winter 2020, by about 0.5–1.5 ppmv, depending on the altitude.

381 The assessment further gives strong evidence that the peak ozone loss in the Arctic winter 2020 is similar to that of the warm

382 winters of Antarctic (e.g. 2019). The loss estimation method can have uncertainty in the range of 3–5%, depending on the

383 winter months. For instance, the monthly mean ozone loss and its standard deviation for each winter month of 2020 are shown

384 in Figure S3. A complete error analyses of the passive method to estimate ozone loss is already presented in Kuttippurath et

385 al. (2010).

386 **3.7 The first appearance of ozone loss saturation in the Arctic**

387 Ozone loss saturation (i.e. O_3 values less than 0.1 ppmv) is a common feature of Antarctic winters since 1987 (Solomon et al.,

388 2005; Kuttippurath et al., 2018; Jin et al., 1996). However, as compared to the Antarctic, the Arctic winters are relatively short

389 (Decembe–March), stratospheric temperatures are about 10 K higher, occurrence of PSCs are infrequent, denitrification is

390 modest and thus, ozone loss is generally more moderate. Therefore, the Arctic never encountered the ozone loss saturation (i.e.

391 the near complete (about 90-95%) loss of ozone at some altitudes in the lower stratosphere between 400 and 550 K) there

before. Apart from these, the vortex-averaged ozone loss normally happens only up to 25–30% in the Arctic winters in accordance with ground-based spectrometer observations and henceforth, a loss saturation was unexpected for Arctic conditions. Figure 5 (right) shows the ozone profile measurements by ozonesondes at two Arctic stations, Alert (82.50° N, 62.33° W) and Eureka (80.05 N, 86.42 W), on selected days. The ozone profiles measured at selected Antarctic stations are also shown for comparisons. In general, the ozone loss saturation in Antarctica occurs at the altitude between 400 and 500 K (e.g. Davis: 68.6°S, 78.0°E and Marambio: 64° S, 56° W), and the altitude range would go up to 550 K for the stations that are always inside the vortex, as shown for Syowa. Note that the ozone loss saturation is taken as 0.2 ppmv and ozone detection limit of sondes is 10 ppbv (Kuttippurath et al., 2018; Solomon et al., 2005; Vömel and Diaz, 2010). The ozone loss observed at Davis and Marambio is always smaller than that at Neumayer, South Pole and Syowa. Therefore, ozone loss saturation is also different at different stations in the Antarctic. Here, the ozonesonde measurements at Alert (on 08 April 2020) show loss saturation at the altitudes 420–475 K (e.g. Wilka et al., 2021). The measurements at Eureka (on 10 April 2020) show loss saturation with about 99% ozone loss at altitudes between 420 and 460 K (see also Bognar et al., 2021). The time series of ozone measurements, as analysed from the available measurements, show that the ozone loss saturation occurred at these stations in early April (Figure S4). The vertical shading in Figure 5 for 0.2 ppmv shows the ozone loss saturation criterion with respect to the ozone volume mixing ratios and the ozonesonde measurements have an uncertainty of 5–10% (Smit et al., 2007). Yet, the ozone measurements at Alert and Eureka are in the saturation limit and thus, provide first evidence for the occurrence of ozone loss saturation in the Arctic. The loss saturation suggests that the Arctic polar stratospheric has entered a newer era of change. Our analyses are consistent with the analyses of Wohltmann et al. (2020), who report about 90–93% loss of ozone in the 450–475 K range in 2020 and with those of Grooß and Müller (2021) who find a lowest simulated ozone mixing ratio of about 40 ppbv in 2020.

3.8 Days with ozone values below a threshold of 220 DU

Since the Antarctic ozone hole is defined with respect to TCO measurements (i.e. below 220 DU), we analysed TCO measurements for the Arctic in 2020, which are shown in Figure 7. It shows the lowest TCO measurements made in the Arctic polar region in the winter of 2020 by three different satellite instruments, OMI, OMPS and GOME. As shown (Fig. 7), the OMI measurements show TCO below 300 DU for almost all winter months inside the vortex, as defined by Nash et al. (1996). The measurements show around 230 DU in early December, about 260 DU in January, about 218–260 DU in February, around 220 DU in March and around 240 DU in April. There are ozone values lower than or equal to 220 DU in early (01–05) December, late (25–26) January, some days (05, 12 and 17–22) in March and few days in early (06–07) April. The occurrences of these low ozone values in December and January are associated with ozone mini-holes triggered by dynamics. However, the appearances of extremely low TOC, below 220 DU, values in March and April are driven by chemistry and this is our topic of discussion. The very low ozone measured by OMI corresponding to the dates are also shown in the ozone maps in the top panel and the exact dates of extremely low ozone occurrences based on OMPS and MERRA-2 data are given in Table S1. The OMPS total column agrees well with that of the OMI measurements throughout the period, where the differences are mostly

425 2–3 DU and are within the uncertainty of both instruments (i.e. about 5–10%). The OMPS measurements have captured all
426 features of OMI measurements throughout the winter. The GOME measurements are very close to the OMI and OMPS
427 measurements too, but are slightly higher in January and February due to the limited coverage of northern polar region by
428 GOME in winter months. As the winter progresses, the GOME coverage improves and therefore, the March and April
429 measurements are in excellent agreement with other satellite observations. The TCO measurements at Alert also manifest the
430 low ozone values of about 200 DU in two days of April; corroborating the satellite observations (Figure 7).
431
432 We also estimated the partial column ozone loss from the ozone profiles of OMPS and MLS satellites (Figure 7, bottom panel).
433 The ozone loss is calculated with respect to the passive method (Feng et al., 2005). The Arctic winters usually show total
434 column ozone (TCO) loss of about 70–80 DU in cold winters, about 45–50 DU in warm winters, and about 90–110 DU in
435 exceptionally cold winters such as in 2005 and 2011 (Goutail et al., 2005; Kuttippurath et al., 2012b; Rex et al., 2005; Manney
436 et al., 2003). The largest column ozone loss ever measured was in the Arctic winter 2011, and was about 110 DU as assessed
437 from all available studies (Griffin et al., 2018; Kuttippurath et al., 2012; Manney et al., 2011). On the other hand, the Antarctic
438 ozone column loss is about twice that of the Arctic, about 150–160 DU, but slightly lower about 100–120 DU in very warm
439 winters (1988 and 2002) and in early years (e.g. 1979–1985) of ozone loss there (Huck et al., 2005; Tilmes et al., 2006;
440 Kuttippurath et al., 2015). The analyses suggest that even the partial column ozone loss in the Arctic winter 2020 is about 115
441 DU at 350–550 K, which is higher than that of the Arctic winter 2011 and similar to that of the loss found in the Antarctic
442 winters 1979–1985, 2002 and 2019.
443
444 Since the ozone loss in the Arctic winter 2020 is up to the levels of that found in some Antarctic winters, we examined the
445 occurrence of extremely low TCO values using data from OMPS and MERRA-2; the results are presented in Figure 8 for
446 selected days. The first appearance of ozone holes in Antarctic winters is also shown for comparison. There are clear and
447 identifiable regions of extremely low TOC (regions below 220 DU) in March and April 2020, which were hundreds of
448 kilometres wide (see also Dameris et al., 2021). The ozone maps show that the low ozone regions in March and April 2020
449 were larger than those measured in the Antarctic in October 1979 and 1980. Therefore, ozone loss in the Arctic winter 2020 is
450 roughly comparable to the Antarctic ozone loss at about 1980. The appearance of a threshold in TCO below 220 DU for several
451 weeks demonstrates that Arctic winters may enter a new era of ozone depletion events, and signal significant changes in the
452 climate of the region (e.g. von der Gathen et al., 2021). However, extremely low TOC values neither appeared in all parts of
453 the vortex nor are present continuously for months as they occur over the Antarctic; further, very strong chemical ozone loss
454 occurs very regularly in the Antarctic, whereas strong Arctic ozone loss occurs only in very cold years (Bodeker et al., 2005;
455 Tilmes et al., 2006; Feng et al., 2007; Müller et al., 2008; von der Gathen et al., 2021).
456
457
458

4. Conclusions

The Antarctic ozone hole has been present for the past forty years, and the impact of ozone hole on public health is mostly restricted to the southern high and mid-latitudes. The ozone hole has also influenced the climate of southern hemisphere by changing the winds, temperature and precipitation in different regions. On the other hand, the biggest concern about the polar ozone loss in the stratosphere has always been strong Arctic ozone loss, because such an ozone reduction can occur anywhere beyond 45° N in the densely populated northern mid and high latitudes. The changes in associated UV radiation incidence would also affect the flora and fauna of the region. If such a situation arose, it would trigger ecosystem damage and impose a serious threat to public health (e.g. Newman et al., 2009). An account of the record breaking increase in UV radiation in the 2019/20 Arctic winter is presented by Bernhard et al. (2020). Nevertheless, it is believed that extreme reductions in column ozone over the Arctic would be unlikely due to relatively higher temperature and a shorter wintertime ozone loss period there. Furthermore, Arctic winters are always prone to several minor and frequent major warmings (almost a major warming per winter), which would restrict the lifetime of the polar vortex, PSC occurrence and chlorine activation to limit the extent and severity of ozone loss. However, the Arctic winter 2020 was exceptional as it was characterised by a strong vortex from December through the end of April, large and widespread PSC occurrence, and unprecedented and prolonged chlorine activation with peak ClO values of about 2.0 ppbv. The high chlorine activation in early December and early January produced larger loss in ozone (e.g. 1–1.5 ppmv below 430 K in early January) in the Arctic that has never occurred before, consistent with the results of the studies of Weber et al. (2021) and Innes et al. (2020). The continued high chlorine activation from January to mid-April caused a record-breaking ozone loss of about 2.5–3.4 ppmv at 400–600 K, and triggered the first-ever observation of extremely low ozone columns in the Arctic in March and April 2020. The unprecedented chlorine activation (e.g. January through March, above 0.7 ppbv) and severe denitrification (60–80%) also set up the atmosphere to have the first ever occurrence of ozone loss saturation in the Arctic. Another interesting aspect of this winter was the dynamically driven but chemically modified ozone mini-holes in December and January. These mini-holes were larger than the Antarctic ozone holes of 1979 and early 1980s. The analyses presented use multiple data sets, different ozone loss estimation methods, and several parameters to make a robust statistics and a balanced assessment of the polar ozone depletion in the Arctic winter/spring 2020.

492 Gathen and Martyn Chipperfield for their help and support in making this article happen. The SLIMCAT forced by ERA5
493 simulation was performed on the University of Leeds ARC4 HPC system.
494

Data availability
496 The MLS data are available on https://disc.gsfc.nasa.gov/. The MODIS datasets were acquired from the Level-1 and
497 Atmosphere Archive & Distribution System (LAADS) Distributed Active Archive Center (DAAC), located in the Goddard
498 Space Flight Center in Greenbelt, Maryland (https://ladsweb.nascom.nasa.gov/). The ozonesonde data are available from the
499 World Ozone and Ultraviolet Radiation Data Centre (WOUDC, https://woudc.org/). The OMPS ozone data are available on
500 https://earthdata.nasa.gov/earth-observation-data/near-real-time/download-nrt-data/omps-nrt. The meteorological analyses:
501 temperature, winds, heat flux, PSC and wave heat flux data are taken from https://ozonewatch.gsfc.nasa.gov/. The OMI data
502 are available on https://disc.gsfc.nasa.gov/datasets/. The GOME data are downloaded from the
503 https://atmosphere.copernicus.eu/data.
504

Author Contributions
506 JK conceived the idea and wrote the original manuscript. The manuscript was subsequently revised with inputs from RM and
507 WF. JK, PK, SR, RR and GK analysed the data and produced the figures. WF designed the model runs and carried out the
508 model simulations. All authors participated in the discussions and made suggestions, which were considered for the final draft.
509

Additional information
511 Supplementary Information accompanies the paper on this journal website.
512

Competing Interests
514 J. K. and R.M. are editors of ACP; otherwise, the authors declare no competing and conflict of interests

References

516 Bai, K., Liu, C., Shi, R. and Gao, W.: Comparison of Suomi-NPP OMPS total column ozone with Brewer and Dobson
517 spectrophotometers measurements, Front. Earth Sci., 9, 369–380. https://doi.org/10.1007/s11707-014-0480-5, 2015.
518 Bai, K., Chang, N.-B., Yu, H. and Gao, W.: Statistical bias correction for creating coherent total ozone record from OMI and
519 OMPS observations, Remote Sensing of Environment, 182, 150–168, 2016.
520 Bais, A., et al.: Environmental effects of ozone depletion, UV radiation, and interactions with climate change: UNEP
521 Environmental Effects Assessment Panel, update 2019, Photochem. Photobiol. Sci., 19, 542–584, 2020.
522 Bernhard, G. H., et al.: Record-breaking increases in Arctic solar ultraviolet radiation caused by exceptionally large ozone
523 depletion in 2020. *Geophysical Research Letters*, 47, e2020GL090844. https://doi.org/10.1029/2020GL090844 ,2020

1

524 Bodeker G. E, Shiona H and Eskes H.: Indicators of Antarctic ozone depletion, Atmos. Chem. Phys., 5, 2603–2615, 2005.

525 Bognar, K., et al.: Unprecedented spring 2020 ozone depletion in the context of 20 years of measurements at Eureka, Canada.

526 Journal of Geophysical Research: Atmospheres, 126, e2020JD034365. https://doi.org/10.1029/2020JD034365, 2021

527 Bojkov, R. D. and Balis, D. S.: Characteristics of episodes with extremely low ozone values in the northern middle latitudes

528 1957–2000, Ann. Geophys., 19, 797–807, https://doi.org/10.5194/angeo-19-797-2001, 2001.

529 Brasseur, G. and Solomon, S.: Aeronomy of the Middle Atmosphere. D. Reidel Publishing Company, Dordrecht, ISBN 90-

530 277-1767-2 (Netherlands), 1984.

531 Bremer, H. et al.: Ozone depletion observed by the Airborne Submillimeter Radiometer (ASUR) during the Arctic winter

532 1999/2000, J. Geophysical Research, 107, 1–7, 2002.

533 Canziani, P. O., Compagnucci, R. H., Bischoff, S. A., and Legnani, W. E.: A study of impacts of tropospheric synoptic

534 processes on the genesis and evolution of extreme total ozone anomalies over southern South America, J. Geophys. Res.-

535 Atmos., 107, 4741, https://doi.org/10.1029/2001JD000965, 2002.

536 Chipperfield, M. P.: New version of the TOMCAT/SLIMCAT off-Line chemical transport model: Intercomparison of

537 stratospheric tracer experiments, Q. J. R. Meteorol. Soc., 132, 1179-1203, doi:10.1256/qj.05.51, 2006.

538 Chipperfield, M. P., et al.: Detecting Recovery of the Stratospheric Ozone Layer, Nature, 549, 211–218,

539 doi:10.1038/nature23681, 2017.

540 Chubachi, S.: Preliminary result of ozone observations at Syowa from February 1982 to January 1983, Mem. Natl Inst. Polar

541 Res., Special Issue, 34, 13–19, 1984.

542 Coy, L., Nash, E. R. and Newman, P. A.: Meteorology of the polar vortex: Spring 1997, Geophys. Res. Lett., 24, 2693–2696,

543 1997.

544 Dameris, M., Loyola, D. G., Nützel, M., Coldewey-Egbers, M., Lerot, C., Romahn, F., and van Roozendael, M.: Record low

545 ozone values over the Arctic in boreal spring 2020, Atmos. Chem. Phys., 21, 617–633, https://doi.org/10.5194/acp-21-617-

546 2021, 2021.

547 DeLand, M. T., Bhartia, P. K., Kramarova, N., and Chen, Z.: OMPS LP observations of PSC variability during the NH 2019–

548 2020 season. Geophysical Research Letters, 47, e2020GL090216. https://doi.org/10.1029/2020GL090216, 2020

549 Drdla, K. and Müller, R.: Temperature thresholds for chlorine activation and ozone loss in the polar stratosphere, Ann.

550 Geophys., 30, 1055–1073, https://doi.org/10.5194/angeo-30-1055-2012, 2012.

551 Dhomse, S. S., Feng, W., Montzka, S. A. et al.: Delay in recovery of the Antarctic ozone hole from unexpected CFC-11

552 emissions, Nat Commun., 10, 5781. https://doi.org/10.1038/s41467-019-13717-x, 2019.

553 Dobson, G. M. B., Harrison, D. N.: Measurements of the amount of ozone in the Earth's atmosphere and its relation to other

554 geophysical conditions: part 1. Proceedings of the Royal Society of London, Series A 110: 660–693, 1926

555 Engel, A., Bönisch, H., Ostermöller, J., Chipperfield, M. P., Dhomse, S., and Jöckel, P.: A refined method for calculating

556 equivalent effective stratospheric chlorine, Atmos. Chem. Phys., 18, 601–619, https://doi.org/10.5194/acp-18-601-2018, 2018.

557 Farman, J. C., Gardiner, B. G. and Shanklin, J. D.: Large losses of total ozone in Antarctica reveal seasonal ClO x/NOx

558 interaction, Nature, 315, 207–210, 1985.

559 Feng, W., Chipperfield, M. P., Davies, S., von der Gathen, P., Kyrö, E., Volk, C. M., Ulanovsky, A. and Belyaev, G.: Large

560 chemical ozone loss in 2004/2005 Arctic winter/spring, Geophys. Res. Lett., 34, L09803, doi:10.1029/2006GL029098, 2007.

561 Feng, W. et al.: Three-Dimensional Model Study of the Antarctic Ozone Hole in 2002 and Comparison with 2000,

562 http://dx.doi.org/10.1175/JAS-3335.1 62, 822–837, 2005.

563 Feng, W., Fast Ozone Loss Around the Polar Vortex During 2002/2003 Arctic Winter Deep Minihole Event, Water, Air, and

564 Soil Pollution, Vol.171: 383-397, 2006.

565 Feng, W., Chipperfield, M. P., Davies, S., Mann, G. W., Carslaw, K. S., Dhomse, S., Harvey, L., Randall, C., and Santee, M.

566 L.: Modelling the effect of denitrification on polar ozone depletion for Arctic winter 2004/2005, Atmos. Chem. Phys., 11,

567 6559–6573, https://doi.org/10.5194/acp-11-6559-2011, 2011.

568 Feng, W., Dhomse, S. S., Arosio, C., Weber, M., Burrows, J. P., Santee, M. L., and Chipperfield, M. P.: Arctic ozone depletion

569 in 2019/20: Roles of chemistry, dynamics and the Montreal Protocol. Geophysical Research Letters, 48, e2020GL091911.

570 https://doi.org/10.1029/2020GL091911, 2021

571 Flynn, L., et al.: Performance of the Ozone Mapping and Profiler Suite (OMPS) products, J. Geophys. Res. Atmos., 119, 6181–

572 6195, doi:10.1002/2013JD020467, 2014.

573 Gelaro, R. et al.: The Modern-Era Retrospective Analysis for Research and Applications, Version 2 (MERRA-2), J. Climate,

574 30, 5419–5454, https://doi.org/10.1175/JCLI-D-16-0758.1, 2017.

575 Goutail, F. et al.: Early unusual ozone loss during the Arctic winter 2002/2003 compared to other winters , Atmos. Chem.

576 Phys., 5, 665–677, doi:10.5194/acp-5-665-2005, 2005.

577 Griffin, D. et al.: Stratospheric ozone loss in the Arctic winters between 2005 and 2013 derived with ACE-FTS measurements,

578 Atmospheric Chemistry and Physics, 19, 577–601, 2019.

579 Griffin, D., Walker, K. A., Wohltmann, I., Dhomse, S. S., Rex, M., Chipperfield, M. P., Feng, W., Manney, G. L., Liu, J. and

580 Tarasick, D.: Stratospheric ozone loss in the Arctic winters between 2005 and 2013 derived with ACE-FTS measurements,

581 Atmos. Chem. Phys., 19, 577–601, https://doi.org/10.5194/acp-19-577-2019, 2019.

582 Grooß, J.-U., and Müller, R..: Simulation of record Arctic stratospheric ozone depletion in 2020. Journal of Geophysical

583 Research: Atmospheres, 126, e2020JD033339. https://doi.org/10.1029/2020JD033339, 2021

584 Huck, P. E., McDonald, A. J., Bodeker, G. E. and Struthers, H.: Interannual variability in Antarctic ozone depletion controlled

585 by planetary waves and polar temperature, Geophysical Research Letters, 32. doi:10.1029/2005GL022943, 2005.

586 Hurwitz, M. M., Newman, P. A., and Garfinkel, C. I.: The Arctic vortex in March 2011: a dynamical perspective, Atmos.

587 Chem. Phys., 11, 11447–11453, doi:10.5194/acp-11-11447-2011, 2011.

588 Inness, A., et al.: Exceptionally low Arctic stratospheric ozone in spring 2020 as seen in the CAMS reanalysis. Journal of

589 Geophysical Research: Atmospheres, 125, e2020JD033563. https://doi.org/10.1029/2020JD033563 ,2020

IPCC. 2007. B. Metz, O.R. Davidson, P.R. Bosch, R. Dave, L.A. Meyer (eds).: Contribution of Working Group III to the Fourth Assessment Report of the Intergovernmental Panel on Climate Change, Cambridge University Press, Cambridge, United Kingdom and New York, NY, USA, 2007.

James PM.: A climatology of ozone mini-holes over the Northern Hemisphere. International Journal of Climatology 18: 1287–1303, 1998.

James PM, Peters D, Greisinger KM.: A study of ozone mini-hole formation using a tracer advection model driven by barotropic dynamics. Meteorology and Atmospheric Physics 64: 107–121, 1997.

Jiang, Y., Yung, Y. L. and Zurek, R. W.: Decadal evolution of the Antarctic ozone hole, J. Geophys. Res., 101, 8985–8999, 1996.

Jin, J. J. et al.: Severe Arctic ozone loss in the winter 2004/2005: observations from ACE-FTS. Geophysical Research Letters, 33, L15801, 2006.

Kirner, O., Müller, R., Ruhnke, R., and Fischer, H.: Contribution of liquid, NAT and ice particles to chlorine activation and ozone depletion in Antarctic winter and spring, Atmos. Chem. Phys., 15, 2019–2030, https://doi.org/10.5194/acp-15-2019-2015, 2015.

Kivi, R. et al.: Ozonesonde observations in the Arctic during 1989–2003: Ozone variability and trends in the lower stratosphere and free troposphere, J. Geophys. Res., 112, D08306, doi:10.1029/2006JD007271, 2007.

Kramarova et al.: Measuring the Antarctic ozone hole with the new Ozone Mapping and Profiler Suite (OMPS), Atmos. Chem. Phys., 14, 2353–2361, https://doi.org/10.5194/acp-14-2353-2014, 2014.

Kroon, M et al.: Comparing OMI-TOMS and OMI-DOAS total ozone column data, J. Geophys. Res., 113, D16S28, doi:10.1029/2007JD008798, 2008.

Krzyścin, J. W.: Long-term changes in ozone mini-hole event frequency over the Northern Hemisphere derived from ground-based measurements. International Journal of Climatology, 22(12), 1425–1439. doi:10.1002/joc.812, 2002.

Kuttippurath, J. et al.: Spatial, temporal, and vertical variability of polar stratospheric ozone loss in the Arctic winters 2004/05–2009/10, Atmos. Chem. Phys., 10, 9915–9930, doi.10.5194/acp-10-9915-2010, 2010.

Kuttippurath, J., A. Kleinboehl, M. Sinnhuber, H. Bremer, H. Kuellmann, J. Notholt, S. Godin-Beekmann, O. P. Tripathi, and G. Nikulin: Arctic ozone depletion in 2002—2003 measured by ASUR and comparison with POAM observations, J. Geophys. Res., doi:10.1029/2011JD016020 (Impact factor 3.826), 2011.

Kuttippurath, J. et al.: Record-breaking ozone loss in the Arctic winter 2010/2011: comparison with 1996/1997, Atmospheric Chemistry and Physics, 2012, 7073–7085, doi.10.5194/acp-12-7073-2012, 2012.

Kuttippurath, J., Lefevre, F., Pommereau, J.-P., Roscoe, H. K., Goutail, F., Pazmino, A. & Shanklin, J. D.: Antarctic ozone loss in 1979–2010: first sign of ozone recovery, Atmos. Chem. Phys., 13, 1625–1635, doi:10.5194/acp-13-1625-2013, 2013.

Kuttippurath, J., Godin-Beekmann, S., Lefèvre, F., Santee, M.L., Froidevaux, L., Hauchecorne, A.: Variability in Antarctic ozone loss in the last decade (2004–2013): high-resolution simulations compared to Aura MLS observations, Atmos. Chem. Phys., 15, 10385–10397, 2015.

1

Kuttippurath, J. et al.: Emergence of ozone recovery evidenced by reduction in the occurrence of Antarctic ozone loss saturation. npj Clim. Atmos. Sci., 1, 42. https://doi.org/10.1038/s41612-018-0052-6, 2018.

de Laat, A. and van Weele, M.: The 2010 Antarctic ozone hole: Observed reduction in ozone destruction by minor sudden stratospheric warmings, Sci. Rep., 1, 38. https://doi.org/10.1038/srep00038, 2011.

Lawrence, Z. D., et al.: The remarkably strong Arctic stratospheric polar vortex of winter 2020: Links to record-breaking Arctic Oscillation and ozone loss. Journal of Geophysical Research: Atmospheres, 125, e2020JD033271. https://doi.org/10.1029/2020JD033271,2020

Livesey, N. J., Santee, M. L., and Manney, G. L.: A Match-based approach to the estimation of polar stratospheric ozone loss using Aura Microwave Limb Sounder observations, Atmos. Chem. Phys., 15, 9945–9963, https://doi.org/10.5194/acp-15-9945-2015, 2015.

Lindenmaier, R. et al.: Unusually low ozone, HCl, and HNO_3 column measurements at Eureka, Canada during winter/spring 2011, Atmos. Chem. Phys., 12, 3821–3835, doi:10.5194/acp-12-3821-2012, 2012.

Lefevre F. et al.: The 1997 Arctic ozone depletion quantified from three-dimensional model simulations, Geophys. Res. Lett., 25, 2425–2428, 1998.

Layola, D. G. et al.: The GOME-2 total column ozone product: Retrieval algorithm and ground-based validation, J. Geophys. Res., 116, D07302, doi:10.1029/2010JD014675, 2011.

Manney G. L. et al. 2011. Unprecedented Arctic ozone loss in 2011, Nature, 478, 469–475,doi:10.1038/nature10556, 2011.

Manney, G. L., Livesey, N. J., Santee, M. L., Froidevaux, L., Lambert, A., and Lawrence, Z. D., et al.: Record-low Arctic stratospheric ozone in 2020: MLS observations of chemical processes and comparisons with previous extreme winters, Geophysical Research Letters, 47. https://doi.org/10.1029/2020GL089063, 2020

Manney, G. L, et al.: Variability of ozone loss during Arctic winter (1991–2000) estimated from UARS Microwave Limb Sounder measurements, J. Geophys. Res., 108(D4), 4149, doi:10.1029/2002JD002634, 2003.

McKenna, D., Jones, R. L., Austin, J., Browell, E. V., McCormick, M. P., Krueger, A. J., and Tuck, A. F.: Diagnostic studies of the Antarctic vortex during the 1987 Airborne Antarctic Ozone Experiment: Ozone mini-holes, J. Geophys. Res., 94, 11 641–11 668, 1989.

Millán, L. F., & Manney, G. L.: An assessment of ozone mini-hole representation in reanalyses over the Northern Hemisphere. Atmospheric Chemistry and Physics, 17(15), 9277–9289. doi:10.5194/acp-17-9277-2017, 2017.

Müller, R., Grooß, J.-U., Lemmen, C., Heinze, D., Dameris, M., and Bodeker, G.: Simple measures of ozone depletion in the polar stratosphere, Atmos. Chem. Phys., 8, 251–264, https://doi.org/10.5194/acp-8-251-2008, 2008.

McPeters, R. D., S. Frith, and G. J. Labow.: OMI Total Column Ozone: Extending the Long-Term Data Record, Atmospheric Measurement Techniques, 8, 4845–4850. doi:10.5194/amt-8-4845-2015, 2015.

Nair, P. J. et al. 2015. Subtropical and mid-latitude ozone trends: implications for recovery, J. Geophys. Res., 7247–7257.

Nash, E. R., Newman, P. A., Rosenfield, J. E. and Schoeberl, M. R.: An objective determination of the polar vortex using Ertel's potential vorticity, J. Geophys. Res., 101, 9471–9478, 1996.

658 Newman, P., E. Nash, and J. Rosenfeld.: What controls the temperature of the Arctic stratosphere during the spring? J.
659 Geophys. Res., 106, 19999–20010, 2001.

660 Newman, P. A., Daniel, J. S., Waugh, D. W. and Nash, E. R.: A new formulation of equivalent effective stratospheric chlorine
661 (EESC), Atmos. Chem. Phys., 7, 4537–4552, https://doi.org/10.5194/acp-7-4537-2007, 2007.

662 Newman, P. A., Lait, L. R. and Schoeberl, M. R.: The morphology and meteorology of southern hemisphere spring total ozone
663 mini-holes, Geophys. Res. Lett., 15, 923–926, 1988.

664 Peters, D., Egger, J., and Entzian, G.: Dynamical aspects of ozone mini-hole formation. Meteorology and Atmospheric
665 Physics, 55(3-4), 205–214. doi:10.1007/bf01029827, 1995.

666 Pitts, M. C., Poole, L. R., and Thomason, L. W.: CALIPSO polar stratospheric cloud observations: second-generation detection
667 algorithm and composition discrimination, Atmos. Chem. Phys., 9, 7577–7589, 2009.

668 Pommereau, J.-P. et al.: Recent Arctic ozone depletion: Is there an impact of climate change?, C. R. Geosci., 350, 347–353,
669 2018.

670 Reed, R. J.: The role of vertical motions in ozone weather relationships, J. Meteorol., 7, 263–267, https://doi.org/10.1175/1520-
671 0469(1950)007<0263:TROVMI>2.0.CO;2, 1950.

672 Rex, M. et al. Arctic ozone loss and climate change, Geophys. Res. Lett., 31, L04116, doi:10.1029/2003GL018844, 2004.

673 Rex, M. et al.: Chemical depletion of Arctic ozone in winter 1999/2000. J. Geophysical Research 107, 8276, 2002.

674 Rieder, H. E., and Polvani, L. M.: Are recent Arctic ozone losses caused by increasing greenhouse gases? Geophys. Res. Lett.,
675 40, 4437–4441, doi:10.1002/grl.50835, 2013.

676 Riese, M., Ploeger, F., Rap, A., Vogel, B., Konopka, P., Dameris, M., and Forster, P.: Impact of uncertainties in atmospheric
677 mixing on simulated UTLS composition and related radiative effects. J. Geophys. Res., 117, D16305,
678 doi:10.1029/2012JD017751, 2012.

679 Rao, J., and Garfinkel, C. I.: Arctic ozone loss in March 2020 and its seasonal prediction in CFSv2: A comparative study with
680 the 1997 and 2011 cases. Journal of Geophysical Research: Atmospheres, 125, e2020JD033524.
681 https://doi.org/10.1029/2020JD033524, 2020

682 Salby, M., Titova, E. and Deschamps, L.: Rebound of Antarctic ozone, Geophys. Res. Lett., 38, L09702,
683 doi:10.1029/2011GL047266, 2011.

684 Santee, M. L., Manney, G. L., Froidevaux, L., Zurek, R. W., and Waters, J. W.: MLS observations of ClO and HNO_3 in the
685 1996–97 Arctic polar vortex, Geophys. Res. Lett., 24, 2713–2716, 1997.

686 Shaw, T. A. and Voigt, A.: Tug of war on summertime circulation between radiative forcing and sea surface warming, Nature
687 Geoscience, 8, 560–566, 2015.

688 Sinnhuber, B.-M. et al.: Arctic winter 2010/2011 at the brink of an ozone hole, Geophys. Res. Lett, 38, L24814,
689 doi:10.1029/2011GL049784, 2011.

690 Sinnhuber, B.-M. et al.: Large loss of total ozone during the Arctic winters of 1999/2000, Geophys. Res. Lett., 27, 3473-
691 3476, 2000.

Sofieva, V. F. et al.: Ozone CCI and OMPS ozone profile dataset and evaluation of ozone trends in the stratosphere, Atmospheric Chemistry and Physics, 17, 12533–12552, 2017.

Solomon, S., Ivy, D. J., Kinnison, D., Mills, M. J., Neely, R. R., Schmidt, A.: Emergence of healing in the Antarctic ozone layer, Science, 353, 269–274, 2016.

Solomon, S., Portmann, R. W., Sasaki, T., Hofmann, D. J. & Thompson, D. W. J. Four decades of ozonesonde measurements over Antarctica. J. Geophys. Res. 110, D21311, 2005.

Sonkaew, T., von Savigny, C., Eichmann, K.-U., Weber, M., Rozanov, A., Bovensmann, H., Burrows, J. P., and Grooß, J. U.: Chemical ozone losses in Arctic and Antarctic polar winter/spring season derived from SCIAMACHY limb measurements 2002–2009, Atmos. Chem. Phys., 13, 1809–1835, doi:10.5194/acp-13-1809-2013, 2013.

Smit, H. G. et al.: Assessment of the performance of ECC ozonesondes under quasi flight conditions in the environmental simulation chamber: insights from the Juelich Ozone Sonde Intercomparison Experiment (JOSIE), J. Geophys. Res., 112, D19306, 2007.

Spang, R., Hoffmann, L., Müller, R., Grooß, J.-U., Tritscher, I., Höpfner, M., Pitts, M., Orr, A., and Riese, M.: A climatology of polar stratospheric cloud composition between 2002 and 2012 based on MIPAS/Envisat observations, Atmos. Chem. Phys., 18, 5089–5113, https://doi.org/10.5194/acp-18-5089-2018, https://www.atmos-chem-phys.net/18/5089/2018/, 2018.

Strahan, S. E. and A. R. Douglass, A. R.: Decline in Antarctic Ozone Depletion and Lower Stratospheric Chlorine Determined from Aura Microwave Limb Sounder Observations, Geophysical Research Letters, 45, 382–390. doi:10.1002/2017GL074830, 2018.

Stenke, A., and V. Grewe: Impact of ozone mini-holes on the heterogeneous destruction of stratospheric ozone, Chemosphere, 50, 177-190, https://doi.org/10.1016/S0045-6535(02)00599-4, 2003.

Steinbrecht, W., Hassler, B., Claude, H., Winkler, P. and Stolarski, R. S.: Global distribution of total ozone and lower stratospheric temperature variations, Atmos. Chem. Phys., 3, 1421–1438 doi:10.5194/acp-3-1421–2003, 2003.

Tilmes, S., Müller, R., Engel, A., Rex, M., and Russell III, J.: Chemical ozone loss in the Arctic and Antarctic stratosphere between 1992 and 2005, Geophys. Res. Lett., 33, L20812, doi:10.1029/2006GL026925, 2006.

Tilmes, S., Müller, R., Salawitch, R. J., Schmidt, U., Webster, C. R., Oelhaf, H., Camy-Peyret, C. C. and Russell III, J. M.: Chemical ozone loss in the Arctic winter 1991–1992, Atmos. Chem. Phys., 8, 1897–1910, https://doi.org/10.5194/acp-8-1897-2008, 2008.

Thompson, D. W. J. and Solomon, S.: Interpretation of recent Southern Hemisphere climate change, Science, 296, 895–899, 2002.

Verhoelst, T. et al.: Metrology of ground-based satellite validation: co-location mismatch and smoothing issues of total ozone comparisons, Atmospheric Measurement Techniques, 8, 5039–5062, 2015.

von der Gathen et al., Nature Comm., 2021.

724 Wargan, K., Kramarova, N., Weir, B., Pawson, S. and Davis, S. M.: Toward a Reanalysis of Stratospheric Ozone for Trend
725 Studies: Assimilation of the Aura Microwave Limb Sounder and Ozone Mapping and Profiler Suite Limb Profiler Data, Journal
726 of Geophysical Research, 125, 1–21, 2020.

727 Weber, M., et al.: Total Ozone Trends from 1979 to 2016 Derived from Five Merged Observational Datasets – The Emergence
728 into Ozone Recovery, Atmospheric Chemistry and Physics, 18, 2097–2117, doi:10.5194/acp-18-2097-2018, 2018.

729 Weber, M., et al.: The unusual stratospheric Arctic winter 2019/20: Chemical ozone loss from satellite observations and
730 TOMCAT chemical transport model. Journal of Geophysical Research: Atmospheres, 126, e2020JD034386.
731 https://doi.org/10.1029/2020JD034386 ,2021

732 Wegner, T., Pitts, M. C., Poole, L. R., Tritscher, I., Grooß, J.-U., and Nakajima, H.: Vortex-wide chlorine activation by a
733 mesoscale PSC event in the Arctic winter of 2009/10, Atmos. Chem. Phys., 16, 4569–4577, https://doi.org/10.5194/acp-16-
734 4569-2016, 2016.

735 Wilka, C., Solomon, S., Kinnison, D., and Tarasick, D.: An Arctic Ozone Hole in 2020 If Not For the Montreal Protocol,
736 Atmos. Chem. Phys. Discuss. [preprint], https://doi.org/10.5194/acp-2020-1297, in review, 2021.

737 Wohltmann, I., Lehmann, R., Rex, M., Brunner, D. and Maeder, J. A.: A process-oriented regression model for column ozone.
738 J. Geophys. Res. 112, D12304, doi:10.1029/2006JD007573, 2007.

739 Wohltmann, I., von der Gathen, P., Lehmann, R. et al.: Near-complete local reduction of Arctic stratospheric ozone by severe
740 chemical loss in spring 2020, Geophysical Research Letters, 47. https://doi.org/10.1029/2020GL089547, 2020.

741 World Meteorological Organization: Scientific Assessment of Ozone Depletion: 2010 (Report 52, Global Ozone Research and
742 Monitoring Project, 2011), 2010.

743 World Meteorological Organization. Scientific Assessment of Ozone Depletion: 2006 (Report 50, Global Ozone Research and
744 Monitoring Project, 2007), 2007.

745 Yamazaki, Y. et al.: September 2019 Antarctic sudden stratospheric warming: Quasi-6-day wave burst and ionospheric effects,
746 Geophysical Research Letters, 47. https://doi.org/10.1029/2019GL086577, 2020.

747 Yang, E.-S., Cunnold, D. M., Newchurch, M. J. & Salawitch, R. J.: Change in ozone trends at southern high latitudes, Geophys.
748 Res. Lett., 32, L12812, 2005.

749 Zhang, J. et al.: Stratospheric ozone loss over the Eurasian continent induced by the polar vortex shift, Nature Communications,
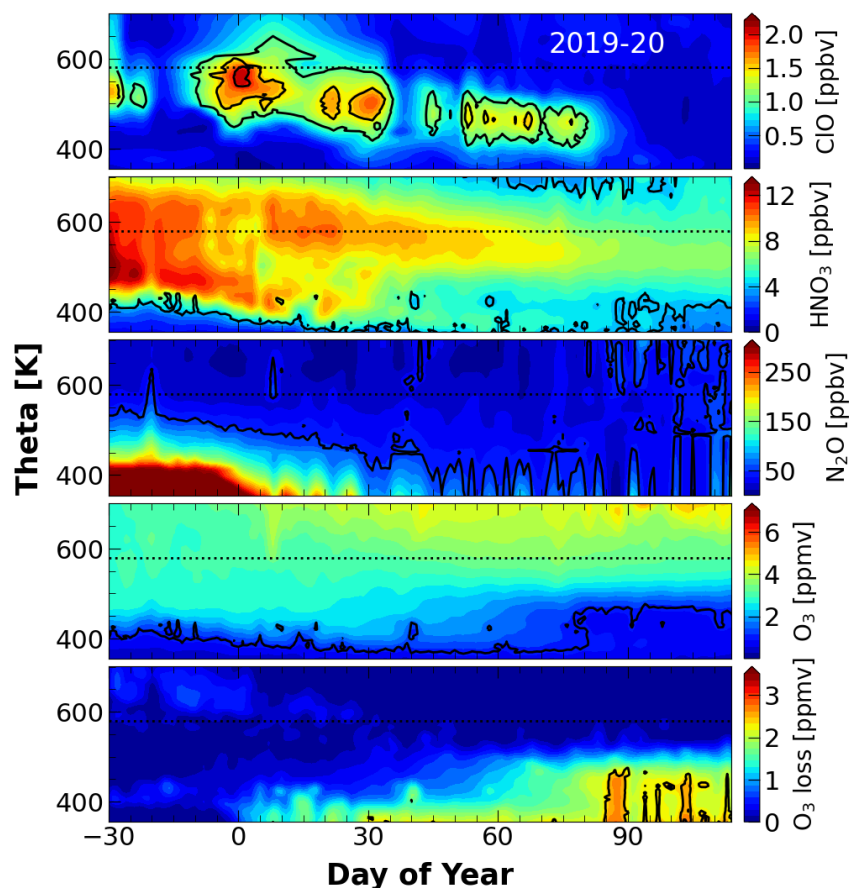750 9, 206, 2018.

751
752
753
754
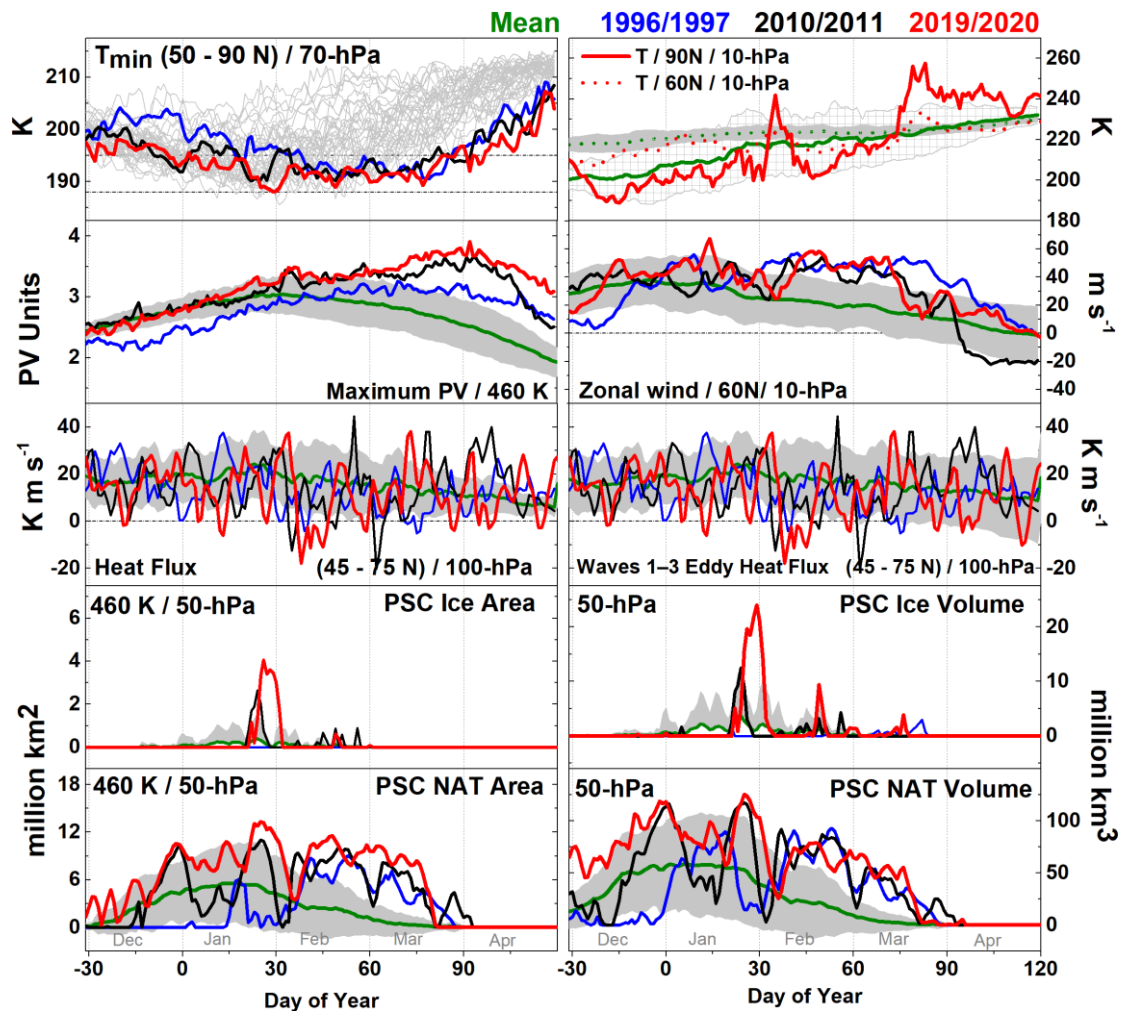
Figure 1: Meteorology of the Arctic winter/spring 2020. The temperature, zonal winds, potential vorticity (PV), heat flux, wave eddy heat flux, and area and volume of polar stratospheric clouds (PSCs) for the Arctic winter 2020 as compared to previous Arctic winters. The shaded area shows the standard deviation from the mean.

755
756
757
758
759
760
761
762
763
764
765
766

1

767
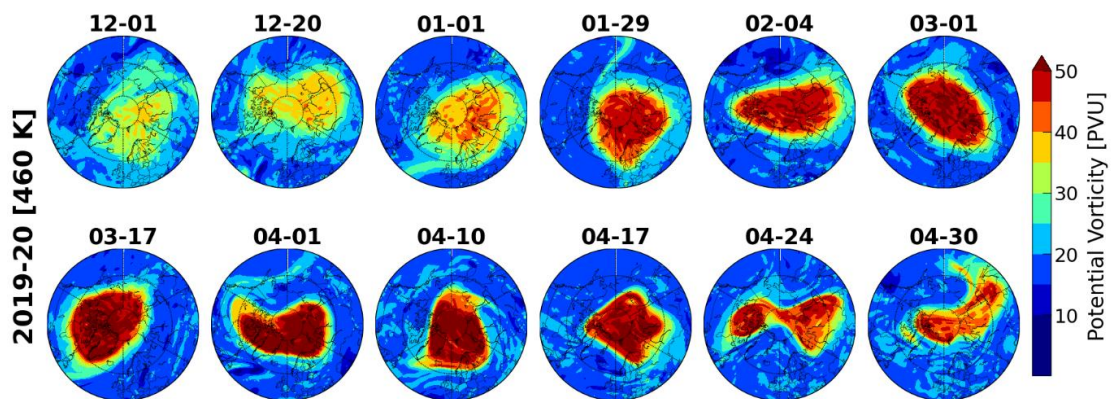
Figure 2: Polar vortex evolution in the Arctic winter/spring 2020. The evolution of polar vortex in the Arctic winter 2020. The vortex situation in the lower stratospheric altitude of about 460 K (~17 km) is illustrated. The vortex edge is calculated with respect to the Nash et al. (1996) criterion at each altitude.

768

769

770

771

772

773

774

775

776

777

778

779

780

781

782

783

784

785

786

787

788

789

790

791

792

Figure 3: Ozone loss in the Arctic polar vortex in 2020. The distribution of ClO, HNO_3, N_2O and ozone (top to bottom) as measured by the Microwave Limb Sounder (MLS) for the Arctic winter 2020. The bottom panel shows the ozone loss estimated using the MLS ozone by applying the tracer descent method (see Methods and supplementary file). The vortex edge is computed in accordance with Nash et al. (1996) criterion. The vortex-sampled data are then averaged over each day and are shown.

801

802

803

804

805

806

807
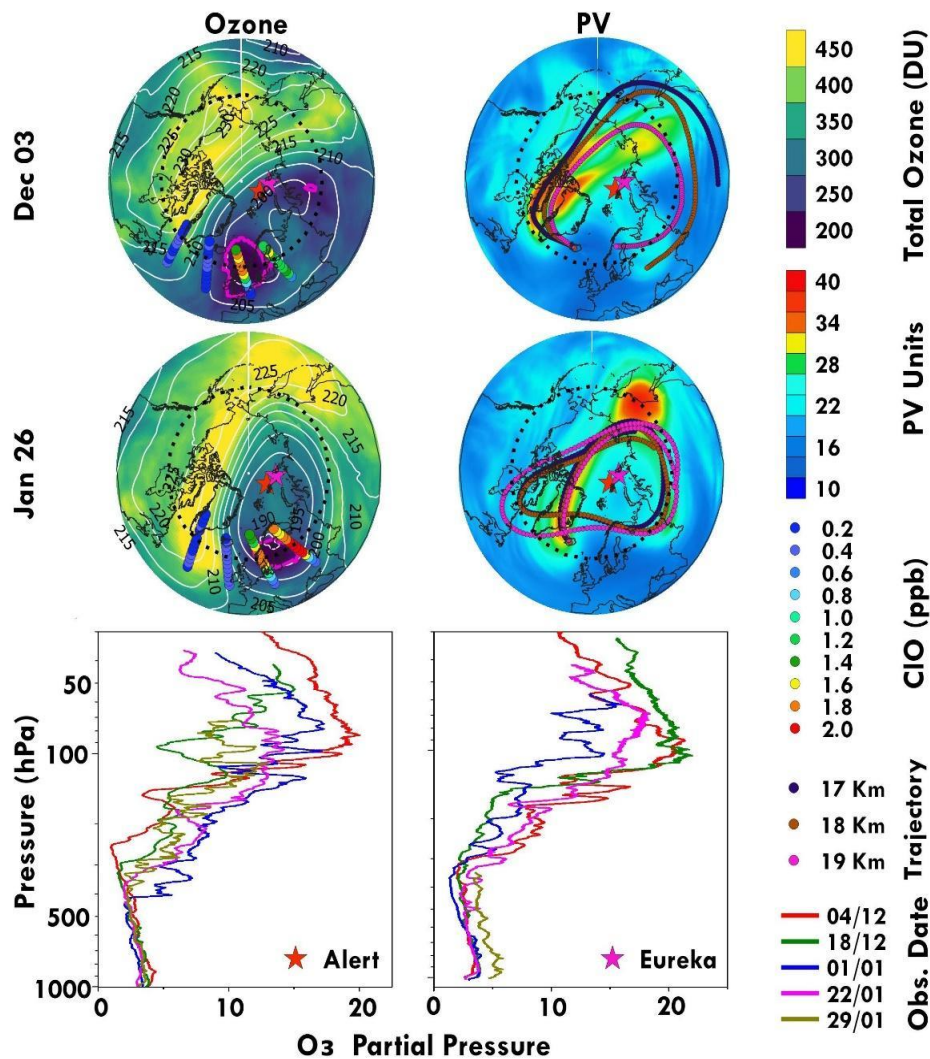
808

Figure 4: The Arctic ozone mini-holes in December 2019 and January 2020. The total ozone observations by Ozone Monitoring Instrument (OMI) on 03 December 2019 and 26 January 2020. The potential vorticity (PV) maps for the corresponding dates are shown on the right. The air mass trajectories computed using the HYSPLIT model at 17, 18 and 19 km are also illustrated in the PV maps. The ozonesonde measurements in December and January at Alert (62.34° N, 82.49° W) and Eureka (79.99° N, 85.90° W) are ilustrated in the bottom panel and are also shown in the maps as red and magenta stars, respectively.

816

817

818
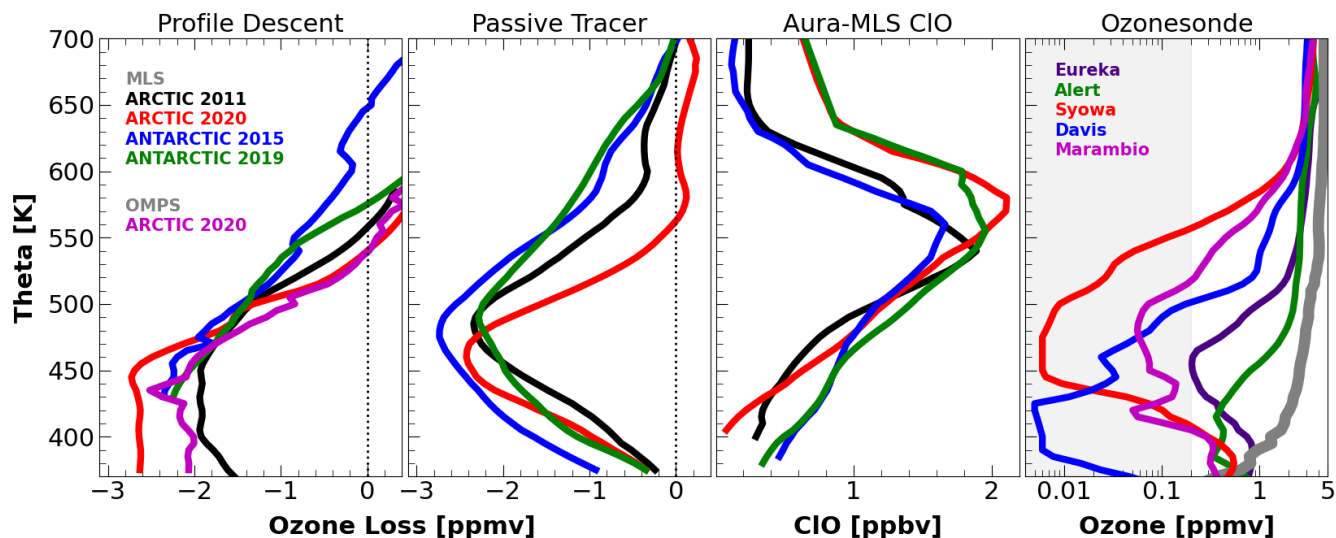
1

Figure 5: The Arctic and Antarctic Ozone Loss Saturation and Chlorine activation. Left. The ozone loss estimated using the Microwave Limb Sounder (MLS) measurements by applying the vortex descent method for the Arctic winter 2019–2020 compared to the Arctic winter 2011, and the Antarctic winters 2015 and 2019. The ozone loss estimated with Ozone Mapping and Profiler Suite (OMPS) measurements is also shown. **Second from the left**: The ozone loss estimated using the passive tracer method for the Arctic winter 2020, and the Antarctic winters 2015 and 2019. **Second from the right**: The activated profiles ClO measured by MLS for the Arctic winters 2011 and 2020, and the Antarctic winters 2015 and 2019. The profiles are selected for the days with peak ClO values and are averaged for three days. **Right:** Ozonesonde measurements from selected Antarctic and Arctic stations. The Antarctic ozonesonde measurements (Davis, Marambio and Syowa) from past winters and the Arctic measurements (Alert and Eureka) from the Arctic winter 2020. The grey colour represents an ozone profile without ozone depletion in Arctic and Antarctic. The grey-shaded region represents the ozone loss saturation threshold. The dates ozonesonde measurements are taken for 08 April 2020 (Alert) and 10 April 2020 (Eureka).
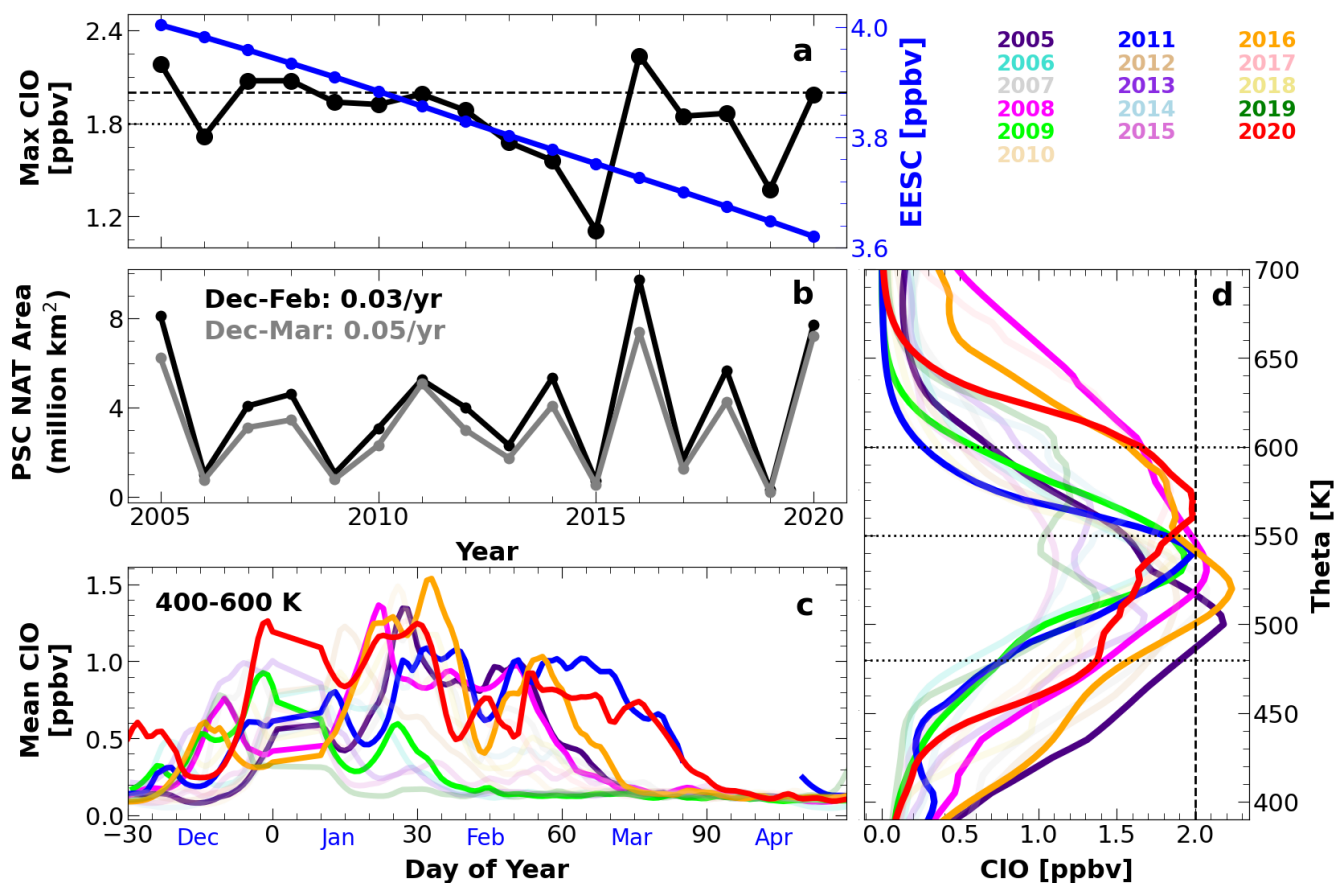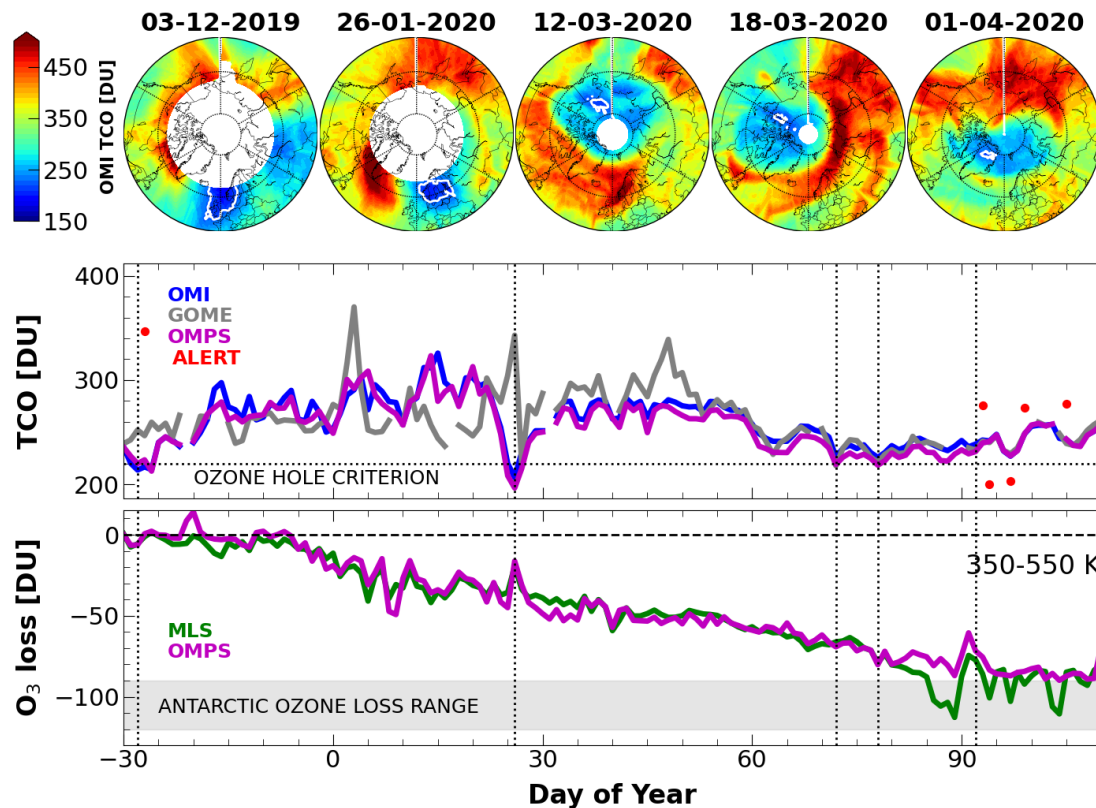
Figure 6: PSC and Chlorine activation the Arctic winters 2005–2020. **(a)** The temporal evolution of ClO in the Arctic winters as measured by the Microwave Limb Sounder (MLS) inside the vortex and Effective Equivalent Stratospheric Chlorine (EESC). **(b)** The Area of PSC averaged for the period December-February and December-March (grey) for the winter since 2005. **(c)** The maximum ClO measured inside the vortex in each winter from 2005 to 2020. **(d)** The maximum ClO profiles measured inside the vortex for Arctic winters since 2005. The high chlorine activation with high ClO values are shown in bright colours and others are faded in (a) and (c). Since the chlorine activation timing is different in different winters, the peak ClO observed between December and April/March are shown.

857

858

859

860

861

Figure 7: Arctic ozone in the total column and partial column ozone. Top: The maps of total column ozone from the OMI satellite measurements in the Arctic for selected ozone hole days for the winter 2020. **Middle panel**: The lowest (5%) TCO measured inside the vortex from three different satellite measurements (OMI, GOME and OMPS). The difference in total column measurements is due to the difference in coverage of the measurements in the Arctic region. The ozone hole criterion of 220 DU is indicated by the dotted line. The total column ozone (TCO) measurements at Alert station are also shown (red solid circles). **Bottom**. The partial column ozone loss computed at the altitude range 350–550 K from the MLS and OMPS measurements. The ozone loss estimated in the Antarctic winters at the same altitude range is shown as the grey-colored area.

862

863

864

865

866

867

868

869

870

871

872
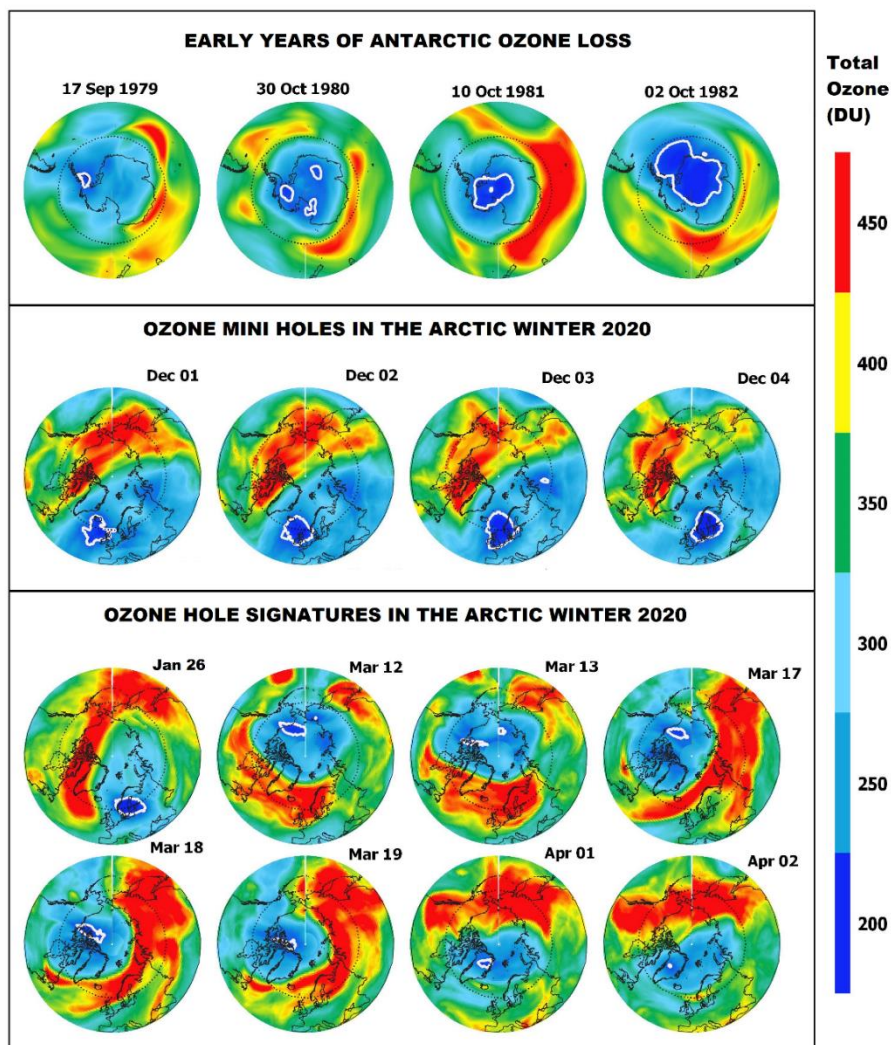
Figure 8: Maps of total column ozone from MERRA-2 and OMPS satellite measurements for selected days. The Antarctic ozone hole is defined as the area below 220 DU of ozone, as demarcated by the white contour. The top panel shows the early years of the Antarctic ozone hole, the middle panel shows the ozone-mini holes driven by dynamics, and the bottom panel shows the ozone column observed in the Arctic winter 2020.

1